

## ANALYSIS OF WEAR AND CORROSION RESISTANCE OF AISI 304 STEEL USED IN COAL MINING

**Abstract:** *The wear and corrosion are phenomenon presents everyday in our life affecting the industries more and more. The stainless steel AISI 304 have a higher resistance to these problems. However isn't exempt from that. Toward better utilization of these material in the coal industry, searching ways to minimize the impact caused by corrosive agents and wear on a centrifugal pumps. Based the problems found, were analyzed some specimen, to verify the stainless steel AISI304 and to discovery out through the differents speeds of the cutting feed which the machining process parameter has a behavior that benefits the material characteristics. Thus making the shaft become more resistance and prolonging the helpful life of the pumps to minimize the charts to maintenance and exchange replacement.*

**Keywords:** *corrosion, wear, stainless steel.*

### 1. INTRODUCTION

In the coal industry, wear and corrosion are phenomena that are present in everyday life, increasingly affecting productivity, thereby decreasing their profit. The centrifugal pump axes, used in mining companies, are subject to these phenomena, due to the extremely aggressive environment to conventional carbon steels. The use of stainless steels is a relatively effective alternative to remedy, in terms, these inconveniences, where austenitic stainless steels are the first alternative for the selection of this class of materials, with characteristics of having high resistance to corrosion.

To contain in your league over 10.5% chromium, and having an adherent and impermeable passive layer that forms on the surface, stainless steel AISI 304 has considerable resistance for corrosion and wear, but with the high level of corrosive agents in the work environment steel has a propensity to lose mass and, as a consequence, gradual wear, thus compromising the useful life of the centrifugal pump shafts.

Machining is one of the most important processes in the manufacture of machine components, where centrifugal pump shafts are included in this context, so it is important to know the effects of this process on the mechanical strength and corrosion resistance of the components, for he manufactured.

### 2. MATERIALS AND METHODS

The material used for the tests was stainless steel AISI 304, obtained from a single bar and formed specimens with dimensions of  $\varnothing$  26 mm and length 110 mm, where in these specimens the machining process was developed with parameters of section described in Table1.

Table 1: cutting parameters applied in the tests

Test	vc [m/min.]	af [mm/rot.]	ap [mm]
1	100	0,1	1,0
2	100	0,2	1,0
3	100	0,3	1,0

The determination of the dimensions of the specimens was based on the useful space on the bench developed for the wear tests of the axes, being defined in a way that made it possible to carry out the roughness measurements, corrosion tests and weighing after the tests.

The machining of the specimens was carried out in conventional lathe and used an interchangeable tool insert TNMG 160408 model TiN coating, and each test piece was machined with different tool cutting edges so as not to compromise the results if there were wear in the same.

To test the veracity of the material used, a metallography test and chemical composition of the steel were carried out.

To perform the metallography, the OLYMPUS BX51M Optical Microscope model was used, and the samples were polished after an electrochemical attack with a 60% NHO<sub>3</sub> and 40% H<sub>2</sub>O solution.

The specimens were subjected to roughness measurements in order to verify the surface characteristics of the parts. For the measurements, the MJ-310 brand SJ-310 rugosimeter was used, with measurement scales used in Ra, Rz and Rt [ $\mu$ m].

The hardness tests were performed with a durometer, for measurement on the Brinell scale [HB] and a microdurometer with Vickers scale [HV], whose method consists in measuring the depth of the impression left on the material with the application of the load.

The wear tests were developed on a bench mounted specially for the simulation test of shaft work in centrifugal pumps. The workbench can be seen in Figure 5, in which it is represented, including, the mechanism of activation of the workbench.

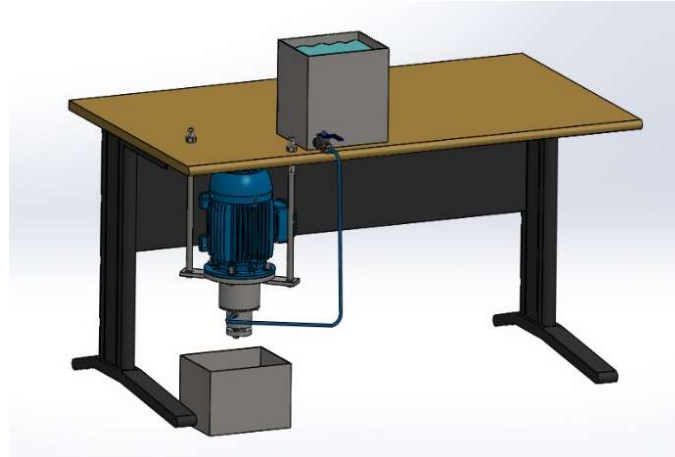


Figure 5. workbench

The motor used to drive the bench, has a power of 5 hp (3.7 kW), three-phase, where a coupling was developed for the interconnection of the motor and the test pieces, a gasket system was also developed and later the superimposed, which serve to maintain the static sealing system and simulate the sealing system of centrifugal pumps that work with this sealing concept, in addition to a 5 liters (5000 ml) container that served as a cooling system and lubrication of the gaskets, where the fluid flow was by gravity. Figure 6 shows, in detail, the sectional representation of the complete mechanism for simulating the wear of axles on pumps.

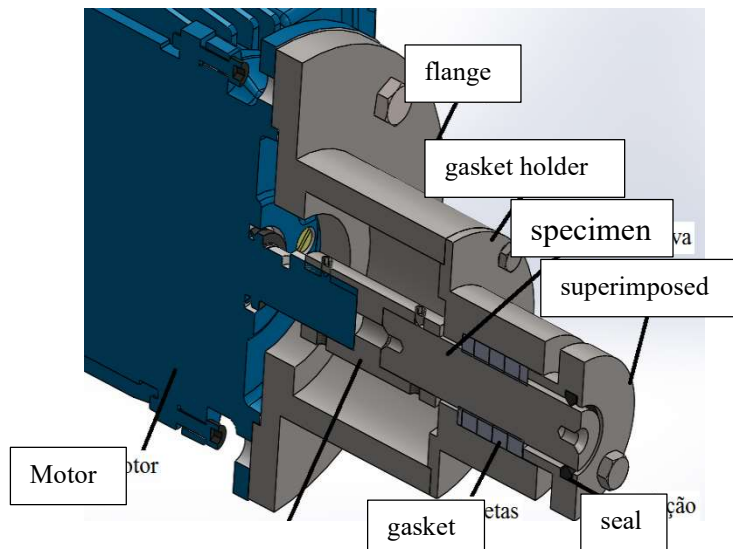


Figure 6. testing device

The wear test was carried out through the friction between the specimens and the gasket sealing system, where they are of the type coated with lubricant (grease), commercially called “graphite acrylic fiber gasket”, the it is recommended for working with centrifugal pumps, withstands temperature variation between -100 and 230 °C, is used in processes with hot or cold water with a minimum pH resistance of 2 and has a speed of 8 m/s.

As the motor speed was 1750 rpm and the diameter of the specimens was 26 mm, the tangential working speed was 2.3 m/s, attesting to be within the product's working range. Equation (A) represents the data needed to find the tangential velocity value of the mechanism.

$$V_p = \frac{\pi \times d \times N}{60000} [m/s] \quad (A)$$

Where:

$V_p$  = peripheral speed [m/s];

$d$  = diameter of the specimen [mm];

$N$  = specimen rotation [rpm];

Another important factor is the pressure exerted by the water inside the gasket system, because depending on the water pressure, a greater or lesser amount of water dripping through the sealing system occurs, which is necessary and determined by the manufacturer of the seals.

Equation (B) shows the value of the pressure determination that occurred during the test, where, as it is an open system, gravity is a determining factor and, therefore, the specific weight of the fluid. As it is a mixture of water with solid elements, the specific weight of the water was adopted, since the other solids were in suspension.

$$P = \gamma \times h \quad (B)$$

Where:

$P$  = pressure [Pa]

$\gamma$  = specific weight of the fluid [N/m<sup>3</sup>]

$h$  = height [m]

The pressure system of work was in the range of 10000 Pa, however converting to a closer unity of the mining sector maintenance system introduced 0.1 bar pressure, this value being within the working range gasket manufacturer that was 15 bar.

The fluid used for the wear test was H<sub>2</sub>O with pH 2, characterizing water as an acidic medium, with addition of mill and magnetite, solid residues in suspension where the mill comes from the extraction of coal and the magnetite is added to the process of coal processing, with 330.49 g of mill and 381.58 g of magnetite for each 5 liters (5000 ml) of water. All solid residues have abrasive characteristics.

The results were validated through the loss of mass of the specimens, obtained in the test benches and finished with the aid of a precision electronic scale model AD500 with weighing capacity between 0.001 to 500 g.

The determination of the intervals between measurements of mass loss was carried out with preliminary tests in an accelerated manner, which reached the value of 10 hours worked to obtain a wear value where it could be measured how much material was removed from the body. of proof. After this preliminary test it was determined that tests would be carried out for 15 hours worked and with interruptions for wear measurement every 3 hours, thus generating a wear trend line of the stainless steel specimen.

After each wear test, a sample was taken from each specimen to perform corrosion tests, and microhardness tests, these samples were Ø 26 mm and 12 mm long. The samples for the accelerated corrosion tests were removed from the regions where there was no wear by contact of the gaskets, see Figure 6, trying during the sample removal, not to heat it, thus avoiding any influence of the temperature in the change of body structure and ensuring the efficiency of the test performed.

For the corrosion tests a bench was made, containing a container with a capacity of 3 liters (3000 ml), and 1.5 liters (1500 ml) of water with pH 2 and 100 ml of HNO<sub>3</sub> nitric acid, a source for the passage of current and conductors, Figure 8 represents the device with the test piece assembled.

The option for acid and the use of the source was due to the verification by ASTM standard, of microstructural analysis of austenitic stainless steels through the use of this acid, as mentioned in the characterization of the specimens, revealing the grain contours, in this way estimated the process of material loss due to corrosion occurs.

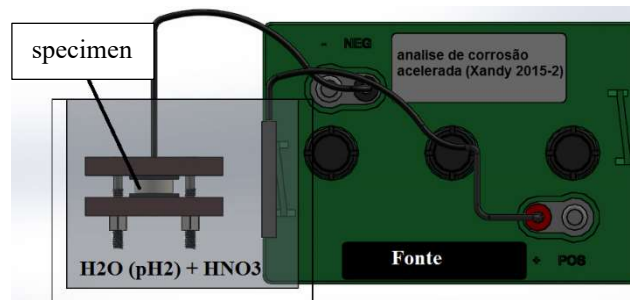


Figure 8. Device for accelerated corrosion testing.

In order to simulate the corrosion process of stainless steel, a period of 5 working hours was determined, where it was possible to clearly verify the corrosion process and the loss of mass, even though knowing that before the mass loss

process, there is the formation of oxides that increase the volume and weight of the material, subsequently generating its removal and loss of mass.

For the superficial visualization of the specimens after the corrosion process, a stereoscope with USB connection.

The use of hand tools and measuring instruments such as calipers and micrometers will not be detailed in this work because it is not the main focus of the work, however they cannot be ignored, as they are extremely relevant to the development of devices and equipment.

### 3. RESULTS AND DISCUSSION

The order of disposition of the results will occur according to the chronological sequence of the tests obtained in the work, where the characterization of the material occurred first.

The Figure 10 shows the result of the electrochemical attack after polishing the sample, where it is possible to be visualized with the aid of the optical microscope.

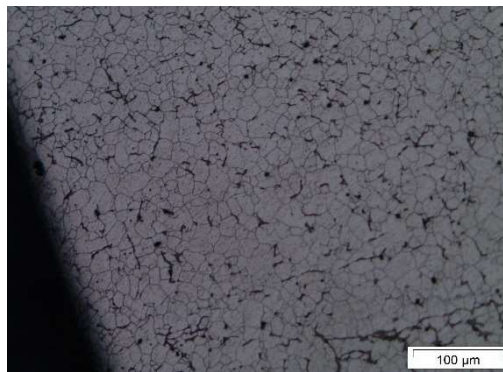


Figure 10. Microstructure of AISI 304 stainless steel

The image indicates the formation of well-defined grains, where through comparison with microstructure books [1], it can be noticed that in addition to the austenitic structure, there are also inclusions in the steel, where they attest that the steel commercially supplied and used for carrying out the assays do not have an established degree of purity.

After the machining of the specimens, with the variation of the cutting parameters described in Table 1, and represented in Figure 11, the roughness measurements were made.



Figure 11. specimen machining

With the production process of the specimens ready, the next step was to carry out the roughness tests, which can be seen in Table 3.

Table 3. Roughness values after machining specimen

Test	Ra [mm]	Rz [mm]	Rt [mm]
1	1,263	8,032	8,684
2	4,401	24,474	25,923
3	7,242	37,41	40,101

According to the roughness results, it can be verified that test 1 obtained lower values of roughness in all conditions of used parameters, while test 3 obtained results inverse to those mentioned above, and intermediate to the two results follows test 2. It can be concluded, preliminarily, that the greater the tool advance during machining, the surface roughness values also increase. As long as the same conditions are maintained for the tests (rotation, depth of cut and radius of the tool tip). Figure 12.

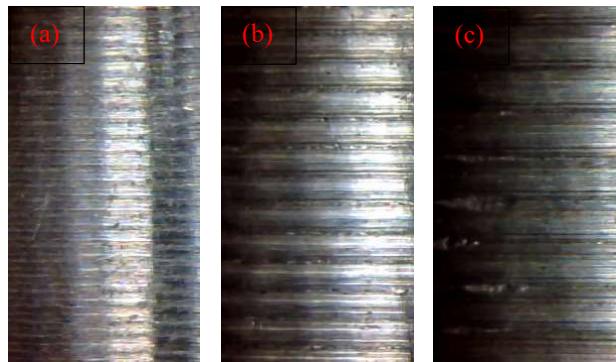


Figure 12. Topography of tests 1, 2 and 3, respectively a, b and c.

Figure 12 represents the results of the machining tests, where the marks of the tools that consequently generated the roughness values can be verified, according to the advances used in the tests.

Figure 13 shows the result of the values obtained in the analysis of mass loss of the specimens, after performing the bench wear tests.

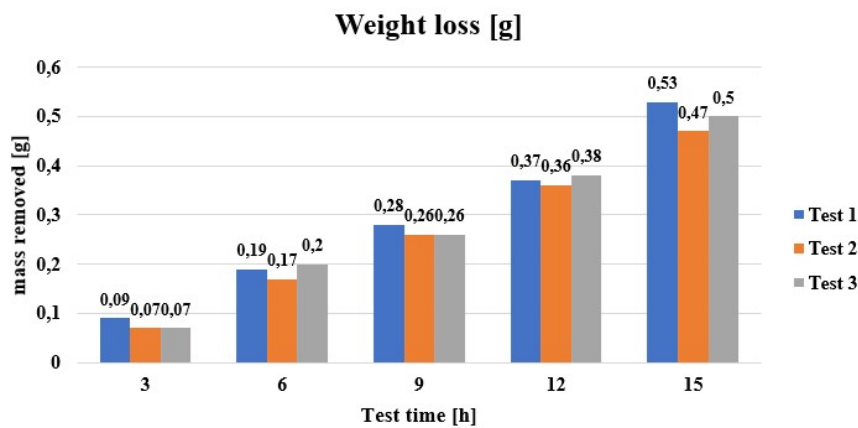


Figure 13. Loss removed

According to Figure 13, it can be seen that test 1 showed a higher wear index in practically the entire test, but it was accompanied by test 2 with values very close to each other. Test 2 was the one with the lowest loss of mass throughout the test, obtaining as the final result the one that behaved better, in relation to all other samples.

The possible justification for the satisfactory result of condition 2, can be better clarified after analyzing the results of the hardness profile found with the performance of the tests on the microdurometer.

Regarding the hardness value on the Brinell scale, the values found were 261 HB using a 2.5 mm carbide sphere and a load of 187.5 kgf.

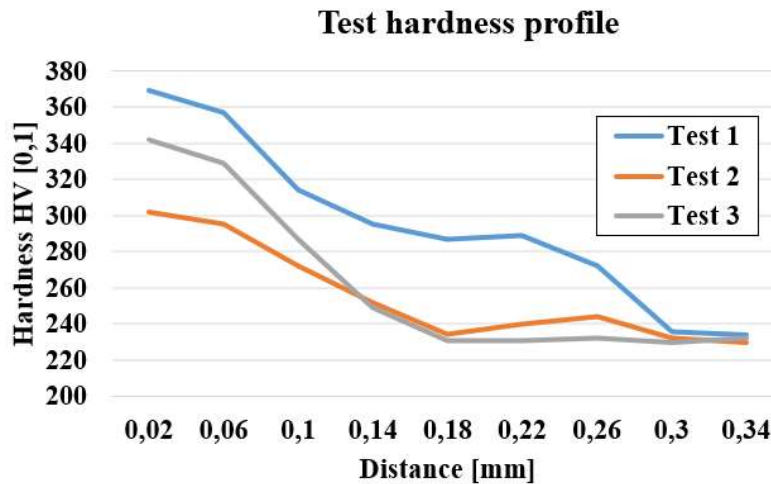


Figure 14. Hardness test

Figure 14 revealed, through the hardness profile graph, that the condition that obtained a lower depth with increased hardness was sample 1, where this fact can be attributed for using a lower tool advance value, exercising a lower effort on the part to be machined, but with a lower roughness value, making the surface more homogeneous, this surface, containing a larger area in contact with the part, thus generating a higher wear value.

In contrast, the surface with the highest roughness value, however with the highest penetration value of the increased hardness was test 3. The reason this sample had a higher loss of mass compared to test 2, can be attributed to a greater number of peaks and valleys on the machined surface, thus, as the area is less in contact with the gaskets of the bench analysis, and the friction force is the same for all samples, the pressure exerted was greater, generating a greater amount of material removed from the test by the abrasion process by three bodies, from the contact between sample / suspended solids / gaskets.

The condition that presented the best performance, among those analyzed, was test 2, which can be attributed to the intermediate value of surface roughness and a hardness profile where it obtained a variation of it until the depth of 0.14 mm, where from this resulted in a stabilization of the average hardness value, while test 3 reached a penetration of 0.18 mm and test 1 stabilized at 0.1 mm.

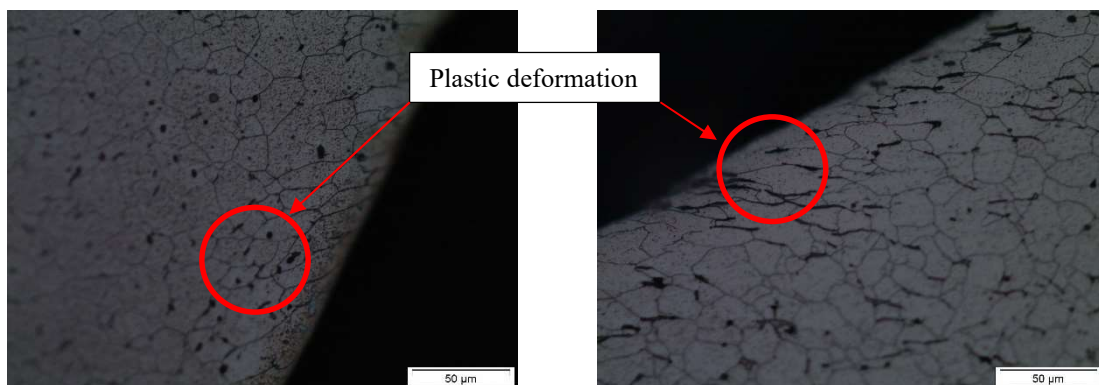


Figure 15 and 16. Test 1 and test 3, respectively

Figure 6 (a) and (b) show the behavior of stainless steel after the machining process with tool feed variation, where it can be seen that sample 3 presented a greater deformation of the grains compared to sample 1, a fact which justifies the variation in hardness of the profiles outlined in figure 6 (a).

The results obtained by the accelerated corrosion test can be seen from Table 2.

According to the results found in Table 2, it can be seen that the test where the greatest increase in mass loss by corrosion was obtained was test 3, followed by test 2 and the test where less mass loss occurred was test 1 .

Table 2. Loss of mass from corrosion

Loss of mass [g]			
Test	Without attack	With attack	Loss of mass
1	43,09	42,87	0,22
2	44,59	44,36	0,23
3	44,95	44,56	0,39

The possible explanation for the occurrence is due to the fact that there is a greater surface roughness, generating greater amounts of peaks and valleys in the topography of the surface of test 3, thus occurring a greater impregnation of impurities with acidic characteristics  $\text{pH} < 4$  originated from the water used added to  $\text{HNO}_3$  acid, further accelerated by the application of electrical current from the source used.

Test 1 showed less loss of mass in relation to all tests, but test 2 with values close to those obtained in test 1, can also be considered satisfactory. The statement is based on the comparison with the values of test 3.

The justification for this increase in mass loss due to the corrosion of the test is due to stainless steel losing its corrosion resistance characteristics when it undergoes plastic deformation, passing its austenitic to martensitic structure, which in addition has magnetic properties.

The results of the corrosion tests of tests 1 and 3 are shown in Figures 7 (a) (b) (c) and (d), respectively, where the difference in texture (roughness) between the condition before the test and after is shown of the test.

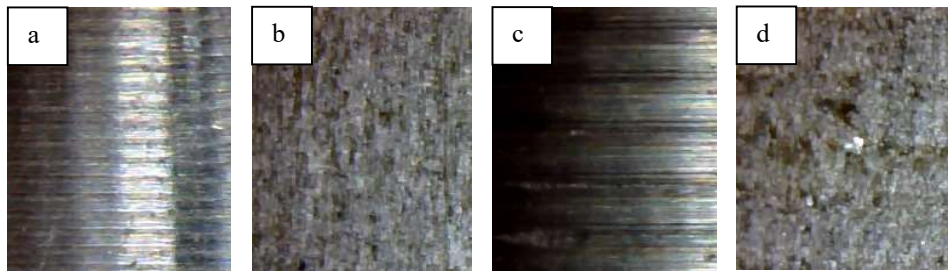


Figure 7. Sample from test 1 before (a) and after (b) the corrosion test and test 3 before (c) and after (d) the corrosion test

It is still noticed that between Figure 7 (b) and (d), all after the corrosion test, the texture of Figure (d) presented a greater roughness, a fact that can be justified by the greater roughness and it is also estimated that there was a greater transformation of the austenitic to martensitic phase, due to the plastic deformation process in the machining of the specimens.

#### 4. CONCLUSION

The cutting advance parameters have a direct influence on the results obtained, both in the wear and corrosion tests. This influence is obtained by the difference in roughness and hardness acquired in the machining of the specimens.

Test 3 was the one with the highest hardness and test 1 the one with the least roughness, however after the wear tests it was notable that the specimen that had a better working condition was test 2, which calls the attention is the fact that this sample is the intermediate sample of the test. Thus, the wear of a part cannot be attributed only to roughness or hardness.

The test bench had satisfactory results, with regard to its operation, as it obtained different results, but consistent with research related to the subjects.

The greater the roughness of the materials, the greater the loss of mass due to the action of corrosive agents, even when using materials with anti-corrosive characteristics.

#### 5. REFERENCES

- [1] PADILHA, Angelo Fernando; GUEDES, Luis Carlos. **Aços inoxidáveis austeníticos: microestrutura e propriedades**. São Paulo (SP): Hemus, 1994. 170 p. ISBN 8528903249.
- [2] JAMBO, Hermano Cezar Medaber; FÓFANO, Sócrates. **Corrosão: fundamentos, monitoração e controle**. Rio de Janeiro: Ciência Moderna, 2009. xxvii, 342 p. ISBN 9788573936810.
- [3] VAN VLACK, Lawrence H. **Princípios de ciência dos materiais**. São Paulo (SP): E. Blücher, 1975. 427 p. ISBN 8521201214.

- [4] DINIZ, Anselmo Eduardo; MARCONDES, Francisco Carlos; COPPINI, Nivaldo Lemos. **Tecnologia da usinagem dos materiais**. 5. ed. São Paulo (SP): Artliber, 2006. 255 p. ISBN 8587296019.
- [5] Silva, F. C. S.; Pereira, J. A.; Ferreira, C. C.M.; Silva, M. B.; **Análise do torneamento do aço inoxidável ABNT 304 através da temperatura do cavaco**. 17º Simpósio do Programa de Pós graduação em Engenharia Mecânica. Uberlândia. 2007.
- [6] CAMPBELL, R. D. Ferritic stainless steel welding metallurgy. **Key engineering materials**, 1992. Apud. SERNA, Carlos Augusto. **Resistência à corrosão intergranular do aço inoxidável ferrítico UNS S43000**: avaliação por método de reativação eletroquímica, efeito de tratamento isotérmico e mecanismo de sensitização. São Paulo, 2006.
- [7] CHIAVERINI, Vicente,. **Aços e ferros fundidos**: características gerais, tratamentos térmicos, principais tipos. 5. ed. ampl. e rev. São Paulo: Associação Brasileira de Metais, 1982. 518p.
- [8] WALLINDER, I. O.; LU, J. ; BERTLING, S.; LEYGRAF, C. **Release rates of chromium and nickel from 304 and 316 stainless steel during urban atmospheric exposure** – a combines field and laboratory study. *Corrosion Science*, v.44, p. 2303-2319, 2002.

#### **RESPONSIBILITY NOTICE**

The author(s) is (are) the only responsible for the printed material included in this paper.